

Optimized Injection Site Location for Magnetic Nanoparticle Induced Hyperthermia Cancer Treatment

BEE 4530 Computer Aided-Engineering: Applications to Biomedical Processes

Biological and Environmental Engineering, Cornell University, Ithaca, NY

Group 01:
Matthew Hall
Dennis Yanga
Kevin Yi
Jiachi Zhou

May 3, 2012



(Attaluri et. al., 2011) [3]

Table of Contents

1. Executive Summary	(3)
2. Introduction	(4)
3. Design Objectives	(5)
3.1 Schematic.....	(5)
4. Results/Discussion.....	(7)
4.1 Solution Optimization.....	(7)
4.2 Sensitivity Analysis.....	(10)
4.3 Validation.....	(12)
5. Conclusions and Design Recommendations.....	(13)
Appendix A: Mathematical Statement of the Problem.....	(15)
Appendix B: Solution Strategy.....	(16)
Appendix C: References.....	(20)

1. Executive Summary

One method of treating cancer, hyperthermia therapy, involves increasing the temperature of tumors above a critical threshold to induce cell death. The specific treatment we are studying involves using magnetic nanoparticles to induce hyperthermia. The nanoparticles are injected directly into the tumor, and the application of a rapidly fluctuating magnetic field heats the nanoparticles. Using this method, only tissues at and immediately adjacent to the injection sites are heated. While the mechanism of hyperthermia therapy has been well characterized, optimizing the therapy is still an area of active research. Many factors such as injection site locations and duration of magnetic field application need to be precisely controlled to maximize damage to cancerous tissue while minimizing damage to benign tissue.

In this project, we modeled the treatment in COMSOL to address these optimization problems. In both the 2D and 3D models, diffusive heat transfer with transient analysis was simulated by COMSOL. For our model, we drafted an irregularly shaped tumor in 2D and an arbitrarily shaped 3D tumor. To model the heating of the tissue, we incorporated specific absorption rate (SAR) approximation to model the collective heating of nanoparticles at the injection sites. The heating of the tumor was implemented via a heat generation term that was dependent on the nanoparticle distribution. We determined that the tumor should be heated above 43 °C but less than 100 °C, and the surrounding healthy tissue should be maintained below 43 °C to prevent unnecessary cell death. Therefore, we defined optimization of the therapy to mean maximization of tumor destruction and minimization of normal tissue damage. We subsequently optimized the solution for heating duration and injection site distribution by minimizing an objective function. Sensitivity analysis was performed on key parameters such as injection location, A , and r_o in order to determine their influence on optimal heating time. We validated the implementation of SAR physics in COMSOL by comparing it to an analytical solution for heating at a point source. Validation of the SAR model against the actual physics of nanoparticle injection is an emerging area of research and beyond the scope of this study.

Our results show that multiple injection sites allow for a more controlled destruction of tissue. The injection site locations were optimized such that the amount of tumor tissue destroyed was maximized and healthy tissue damaged minimized. Single injection sites are limited to a spherical distribution of nanoparticles and therefore a spherical area of tissue ablation. We also determined that increasing values of A and decreasing r_o , which relates to increased injection concentrations, greatly reduces the time of heating required to bring the tumor tissue to the desired temperature. The location of the injection site was the most important factor to consider in optimization.

The significance of this research is that magnetic nanoparticle hyperthermia treatment can benefit from this precise engineering transport model to achieve greater effect. More specifically,

in clinical settings, this model may aid physicians in determining optimal injection sites and treatment length, and improve the overall prognosis for patients.

2. Introduction

Cancer is a disease characterized by uncontrolled and unregulated cell growth. The growing cells form malignant tumors and spread to nearby and/or distant healthy tissue sites. When left untreated, cancer will cause the eventual death of the patient. Cancer is currently the second most common cause of death in the U.S. The American Cancer society estimates that about 1,638,910 new cancer cases are expected to be diagnosed in 2012, and about 577,190 Americans are expected to die of cancer [1]. Presently, there are a number of ways to treat malignant cancer: surgical removal of bulk tumor, chemotherapy, and radiation therapy are currently highly utilized therapies [1]. Most regimens utilize a combination of aggressive targeting of the bulk tumor and prevention of the spread of metastasizing tumor. However, most of these cancer therapies are either highly invasive or result in undesirable side effects. Hyperthermia therapy has recently gained some attention as a viable cancer treatment due to its relatively low risk, low cost, ease of implementation, and minimal side effects. Therefore, hyperthermia therapy garners further research into its potential in becoming a cancer treatment of choice.

Previous studies have shown that localized hyperthermia therapy using magnetic nanoparticles was successful in killing tumors in clinical and preclinical tests [2]. The nanoparticles that were used in their study, iron oxides magnetite (Fe_3O_4) and maghemite $\gamma\text{-Fe}_2\text{O}_3$, are shown to be biocompatible in human tissue [7]. The experiment involved injecting the nanoparticles into the surrounding tumor extracellular space at single and multi-injection sites. A magnetic field was then applied to excite the nanoparticles to stimulate localized hyperthermia within the tumor [3]. The application of a rapidly fluctuating magnetic field heats the nanoparticles, effectively heating the tumor in localized regions while minimizing over-heating of surrounding healthy tissue. Studies have also reported that the duration of heating, also known as thermal dose, and the distribution of the nanoparticles both have tremendous influences on the effectiveness of the treatment [4,5].

The aim of this project was to optimize the distribution of nanoparticles and the thermal dose to effectively kill the bulk tumor while concomitantly minimizing damage to the surrounding healthy tissue. We will model the magnetic nanoparticle heating of 2D and 3D tumor geometries and determine the effect of various parameters on the efficacy of the treatment. Our goal is to be able to identify the parameters that play the greatest role in optimization and how one might systematically be able to determine the best possible combination of those parameters to minimize healthy tissue loss and offer the best outcome for the patient. Consistent with our aim, our design objectives are:

3. Design Objectives

- Reach a specific threshold temperature ($> 43 \text{ }^\circ\text{C}$) inside the tumor to kill tumor cells
- Minimize damage to surrounding healthy cells ($< 43 \text{ }^\circ\text{C}$)
- Minimize excessive heating to all cells ($< 100 \text{ }^\circ\text{C}$)
- Determine the parameters needed to optimize the treatment such as:
 - Injection site locations
 - Thermal dose
 - Maximum specific absorption rate
 - Nanoparticle distribution distance from center of injection

3.1 Schematic

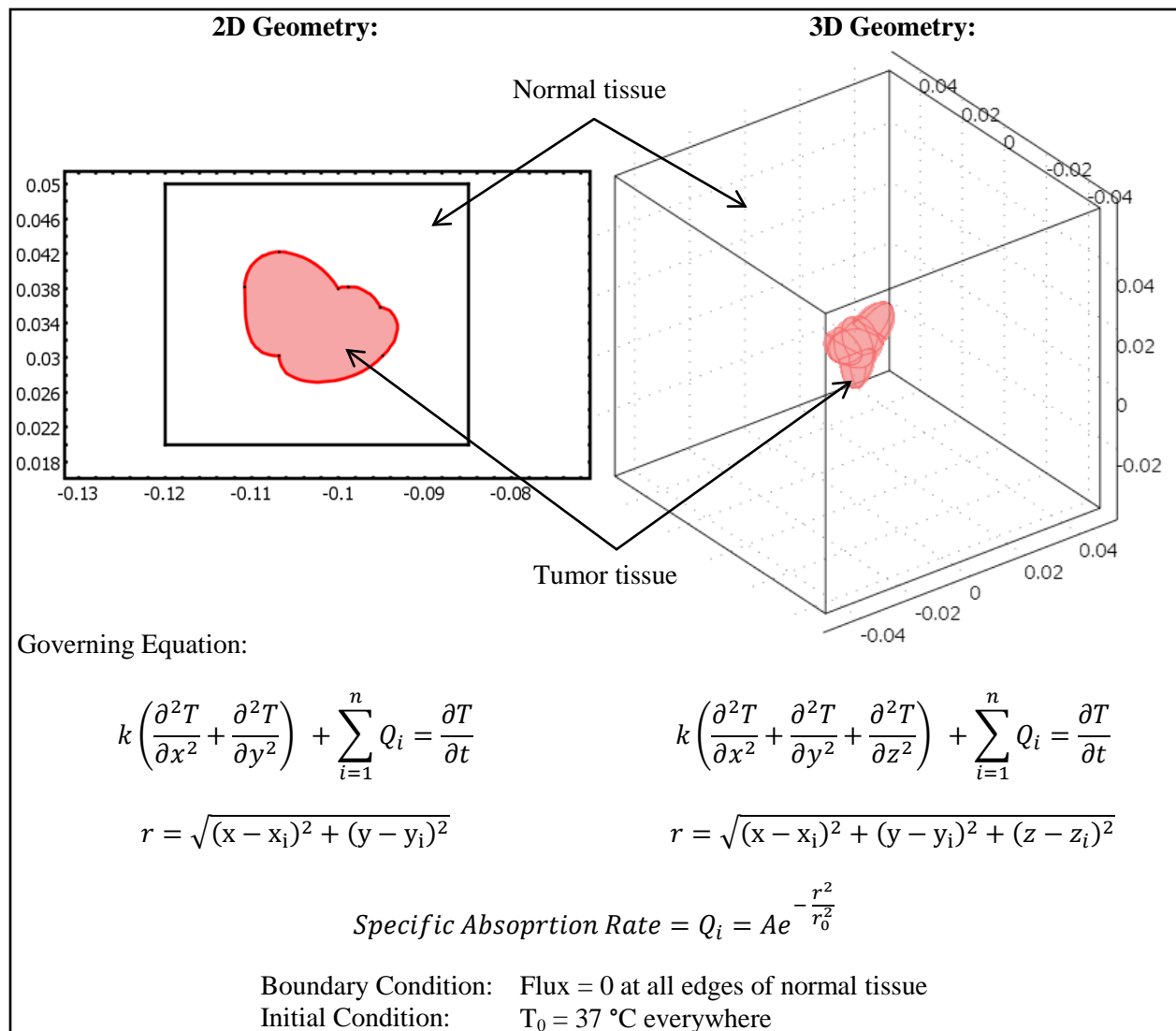


Figure 1: Schematic of the 2D and 3D geometries used to simulate tumor tissue. The x , y , and z axis of each model is in units of meters. The governing equations used are the 2D and 3D heat transfer equations with the conduction, transient, and heat generation terms.

In both the 2D and 3D models, the geometry of the tumor was set arbitrarily to demonstrate each model's ability to predict the temperature profile for any tumor geometry. The size of the simulated tumor tissues are on the length scale of realistic cancer tumors (approximately 2 cm). The governing equation used in each model is the heat transfer equation which includes the conductive, generation, and transient terms. Each injection site acts as a source of the heat generation term, which is given by the specific absorption rate (SAR) (Appendix A). The particles were assumed to be static once injected into the tumor cells so that mass transfer could be neglected in this model.

Injecting magnetic nanoparticles at a single injection site gives little control of the temperature distribution within an irregularly shaped tumor (Figure 2A). In contrast, if there are multiple injection sites, volumetric heating at a point is the sum of the heating term from each injection site (Figure 2B). This effect allows for precise shaping of the temperature distribution within the tissue to destroy a tumor of irregular geometry while leaving the surrounding normal tissue undamaged.



Figure 2: Schematic showing tumor geometry and location of (a) single injection site and (b) multiple injection sites. At a point (x, y) the volumetric heating term, Q , is a sum of the exponential distributions from each injection site I_1, I_2, I_3 .

4. Results/Discussion

4.1 Solution Optimization

We determined the optimal location for the injection sites by minimizing an objective function (J). This function was set such that elements inside the tumor which are below 43 °C increase the value of the function and elements outside the tumor which are above 43 °C also increase the value of the function, but to a lesser extent (see below).

$$J = \sum_i F_{Tumor}(T_i) + \sum_j F_{Healthy}(T_j)$$
$$F_{Tumor}(T) = \begin{cases} 10, & T < 43 \\ 0, & 43 \leq T < 100 \\ 10000, & T \geq 100 \end{cases}$$
$$F_{Healthy}(T) = \begin{cases} 0, & T < 43 \\ 1, & 43 \leq T < 100 \\ 10000, & T \geq 100 \end{cases}$$

Here we place a greater importance on destroying the tumor tissue over protecting the surrounding normal tissue by weighting a given volume of tumor tissue below 43 °C ten times more than the same volume of normal tissue above 43 °C. Above 100 °C the tissue will begin to boil causing catastrophic injury to the patient, so any volume above 100 °C was given an extremely high weight of 10000.

A 2D transient solution was performed in COMSOL as a preliminary study to determine how long the magnetic field should be continuously applied to induce the desired temperature of 43 °C throughout the entire tumor interior.

Optimized 2D solution

Three injection sites were arbitrarily placed in the 2D tumor geometry evenly spaced from the boundaries. The location of each injection site was then adjusted in 2 mm increments and the solution for every combination of injection site locations was found. The optimal injection site locations were found using the objective function discussed previously (Figure 3).

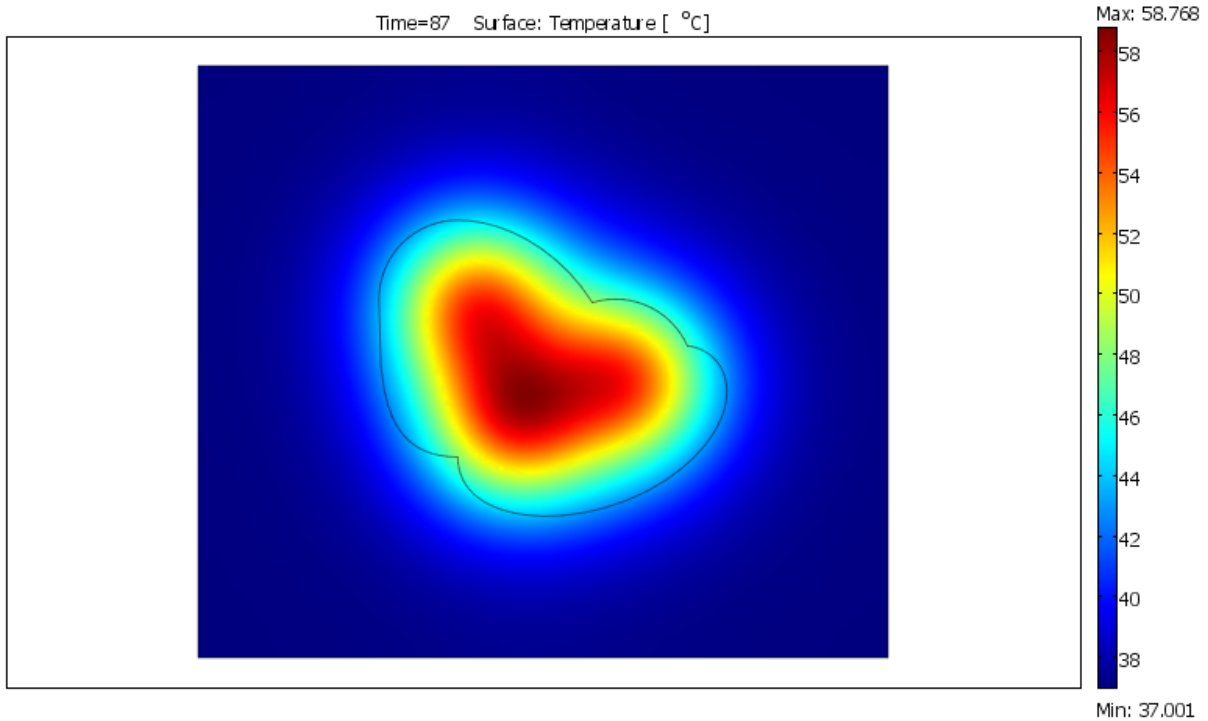


Figure 3: Surface plot of the 2D tumor geometry with optimized injection site locations. The ideal heating time (87 s) corresponds to the maximum amount of tumor destroyed and minimal damage to healthy tissue.

For the optimized 2D solution, 0.156 % of the original tumor area was not heated above the therapeutic temperature and thus survived. In contrast, the amount of healthy tissue killed was equivalent in size to 16 % of the original tumor area.

It would seem that the 2D solution provides a good estimate for optimal injection location and treatment time. However, a 3D representation would better capture the geometry of an actual tumor and thus would provide a more accurate result.

Optimized 3D

A single injection site location was initially chosen in our 3D model. After heating for two and a half hours, the entire tumor was not yet heated to the target therapeutic temperature of 43 °C, which indicated that tumor injection site optimization was important to improve therapeutic efficiency. Furthermore, the result indicated that optimization of the solution required multiple injection sites.

The locations of 4 injection sites within the tumor were optimized using the objective function. This was achieved through fixing 1 injection site to the tumor's center of mass and setting the other 3 injection sites somewhere along the major axis of each ellipsoid arm.

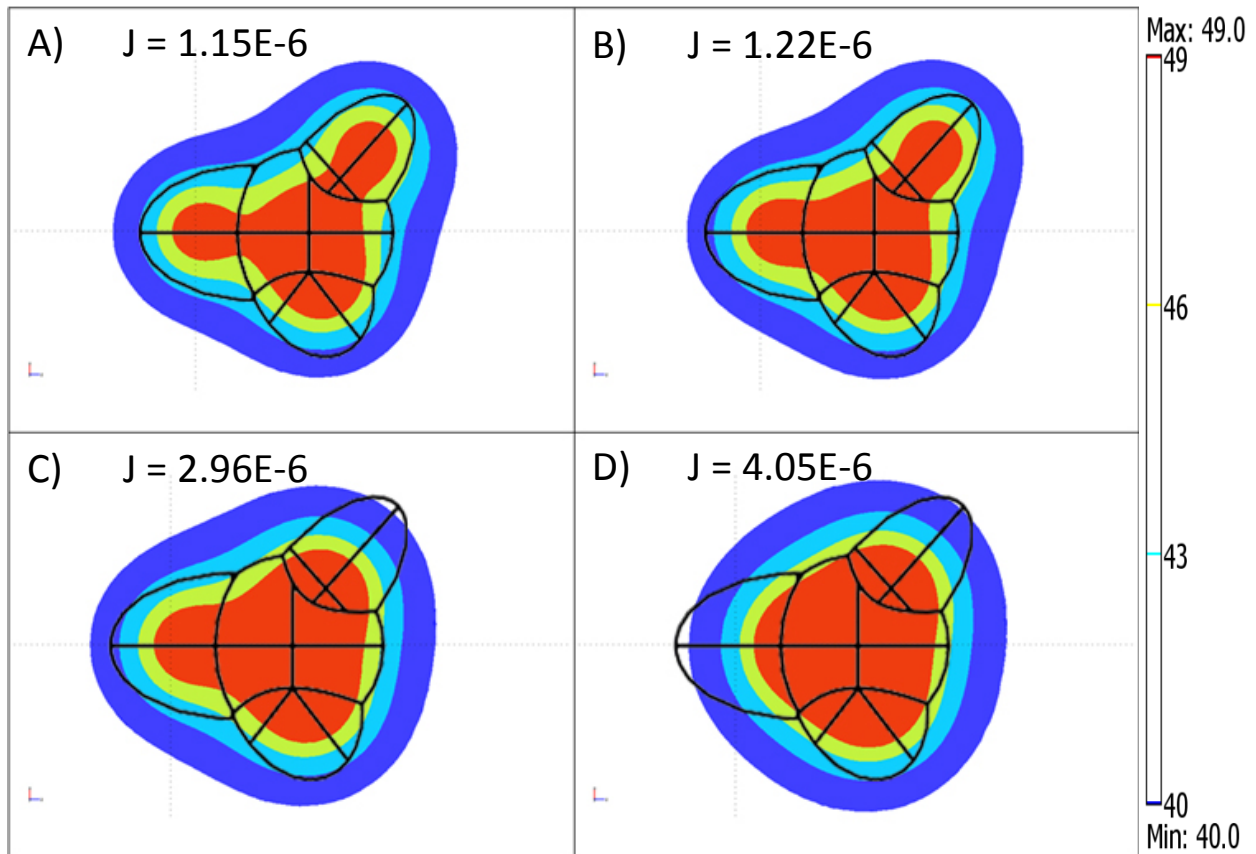


Figure 4: Contour plots of the A) fine optimized solution, B), C), D) coarse optimized solutions for different objective function values. The target temperature of 43 °C is just barely achieved at the outermost points of each tumor arm.

A coarse optimization was first performed for the location of the 3 injection sites in each of the ellipsoid tumor arms. The injection sites were determined by moving out from the center of each ellipsoid along the respective major axis in 2 mm increments. The objective function was then evaluated at each of the 27 possible injection site combinations. The optimal injection site locations were determined to be the coarse optimization with the minimum objective function value of 1.22E-06. We subsequently performed a fine optimization around the solution for the coarse optimization to refine the location of the optimal injection sites. This was done by considering 3 additional injection sites in each tumor arm: one at the previous optimal location, one 1 mm closer to the tumor center along the ellipsoid axis, and one 1 mm farther away. The new optimal locations for the injection sites were found with a new minimum value of the objective function of 1.15E-06 (Figure 5). After heating for 306 seconds, the refined optimal location has only 0.45 % of the tumor volume below 43 °C and 35 % of the tumor volume of the normal tissue above 43 °C (Figure 4). This was compared to the heating for 297 seconds, which yielded in 0.87 % of the tumor volume below 43 °C and 33 % of the tumor volume of the normal tissue above 43 °C for the original coarse solution.

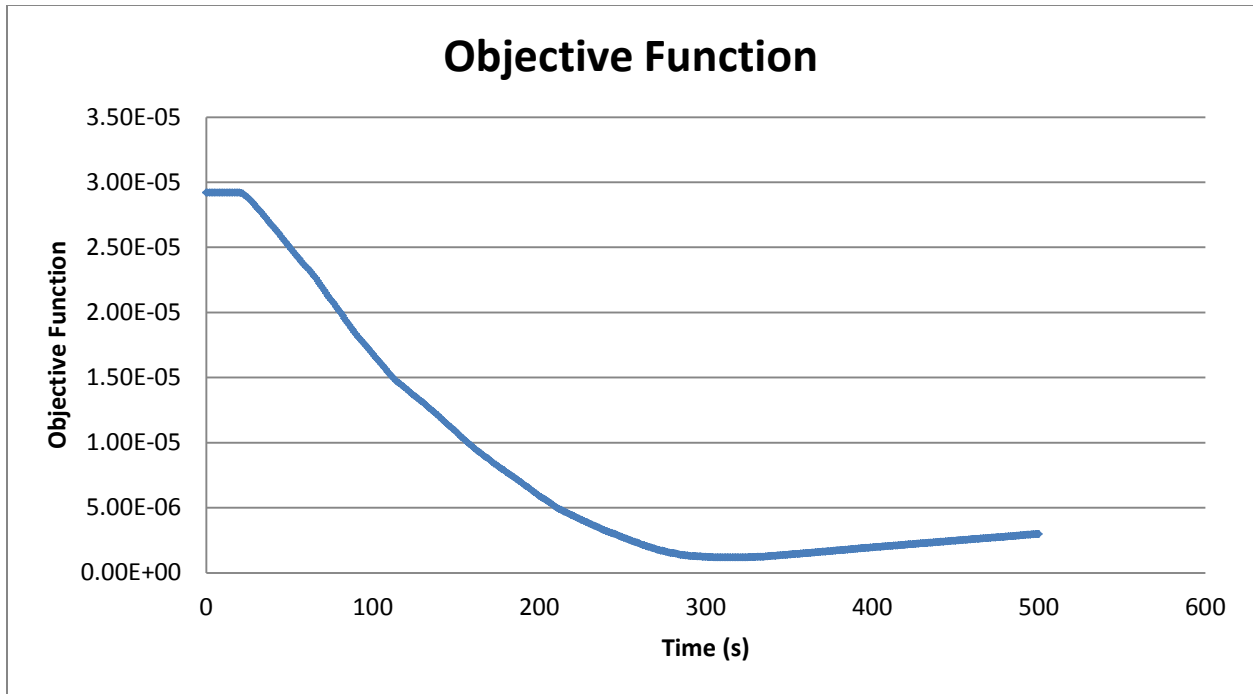


Figure 5: Plot of normalized objective function for the optimized solution. The objective function is minimized at 306 seconds.

4.2 Sensitivity Analysis

The sensitivity of the optimal heating time to A and r_o was computed for the 3D tumor geometry with optimal injection site locations ($J = 1.15E-6$). For both A and r_o a parametric sweep of 10 values ranging from half to double of the original literature values was performed and the corresponding optimal heating time was recorded for each value (Figure 6).

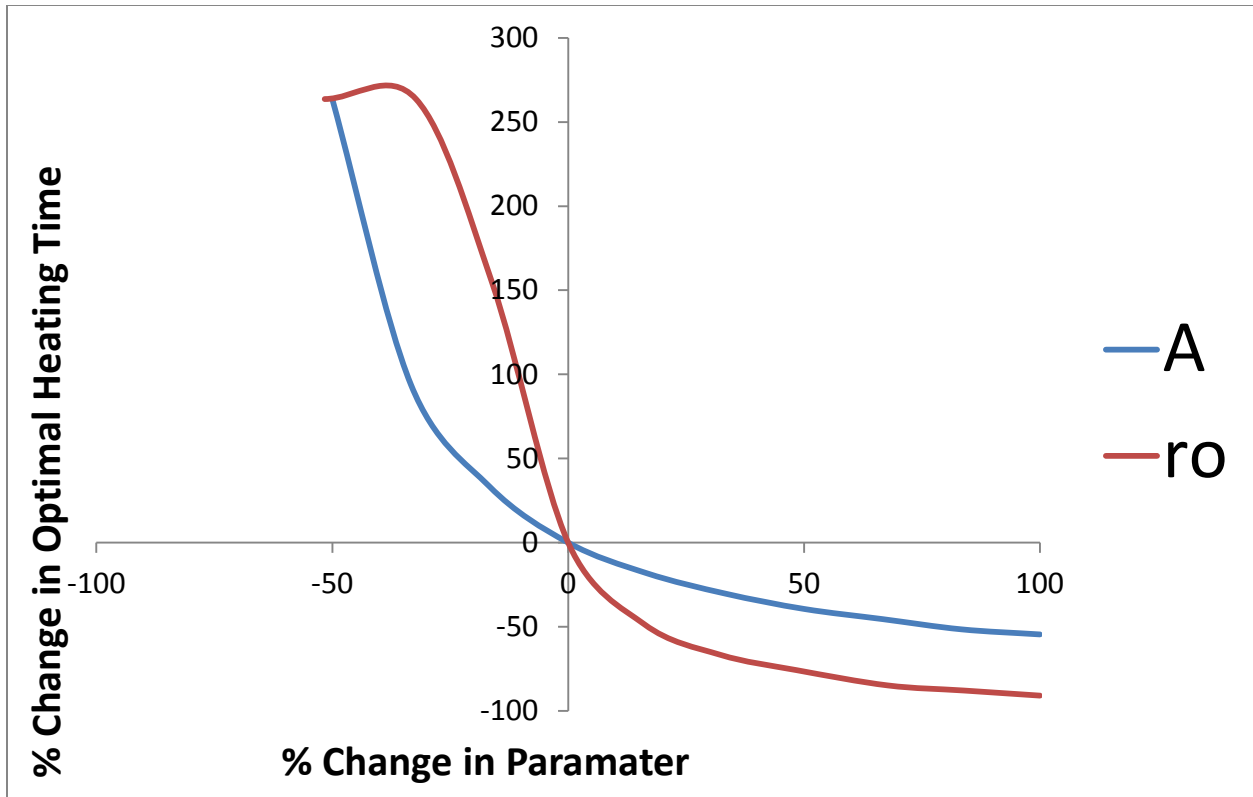


Figure 6: Sensitivity of optimal heating time to parameters A (blue) and r_o (red). The optimal heating time is extremely sensitive to changes in r_o (e.g. 13 % decrease in r_o increases the optimal heating time by about 120%).

These results indicate that the model is highly sensitive to the SAR parameters as a 16 % increase in r_o results in over a 100 % increase in the heating time required to achieve a similar level of hyperthermia treatment. Since this parameter is related to the injection rate and concentration of nanoparticles, great care must be taken when injecting the nanoparticles since even a slight amount of variability can have a large impact on the optimal therapy duration.

4.3 Validation

To validate that COMSOL was correctly implementing the specific absorption rate heating model in the vicinity of each injection site, we compared the COMSOL solution to a similar analytical solution at steady state. In COMSOL, a single injection site was placed in the center of a large domain with constant temperature (37 °C) boundary conditions. The problem was then solved at steady state. This COMSOL solution for heating from an injection site was compared to the known steady state analytical solution for a point emitting a constant heat flux:

$$T = \frac{Q_{tot}}{4\pi kr} + T_{\infty}$$

Where T is the temperature, Q_{tot} is the total power output, k is the thermal conductivity, r is the distance away from the point source, and T_{∞} is the temperature far away from the heat source.

In order for the two solutions to be directly comparable, the total power output of the point source was set equal to the total power output of one injection site. The total power output of a single injection site was calculated by calculating the triple integral of the volumetric heating Q with respect to each of the 3 spatial coordinate direction with integration bounds equal to the domain size (numerical integration using the `triplequad()` function built into MATLAB). Using this method the total power was found to be 0.317 W. This result was verified in COMSOL by placing a single injection site in a domain with 0 flux at the boundaries. With a 0 flux boundary condition the total energy input into the system by the injection site heating is equal to the thermal energy stored by the system. Knowing the heating time of the COMSOL solution, the power output of a single injection site was found to vary less than 2 % from the integral solution verifying that this is the correct answer.

A plot of steady state temperature vs. distance from the inject site/point source was produced for both the COMSOL solution for a single injection site and the analytical solution for a point source with identical total power output to one injection site (Figure 7). The solutions are in close agreement having similar distributions. Some variation in the solutions is expected because in the injection site case the heating is spread over a larger area than for the point source. Indeed, the temperature near the heating source is slightly greater for the point source because of the greater concentration of heating. Overall, the two solutions are sufficiently similar to validate COMSOL's implementation of the Specific Absorption Rate Model physics.

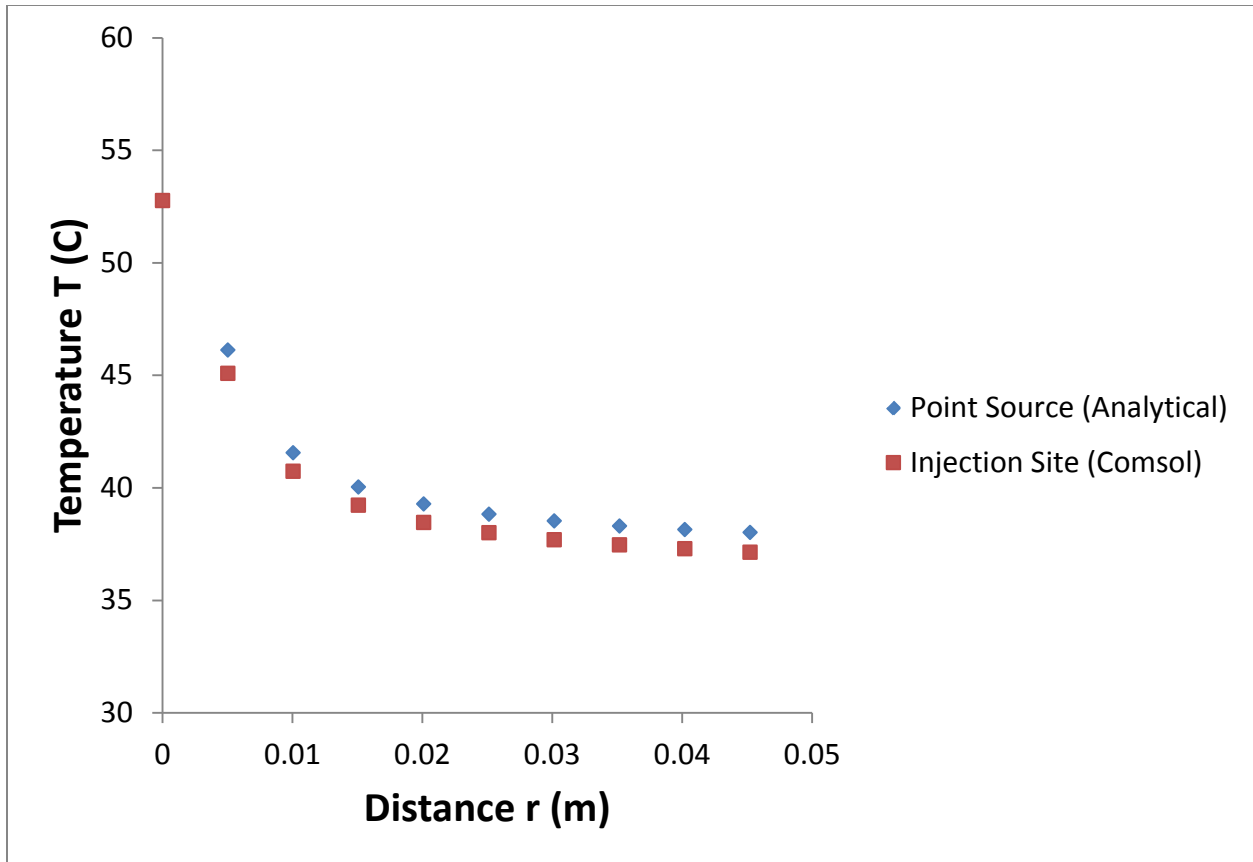


Figure 7: Validation of the specific absorption rate heating model physics implementation in COMSOL. The steady state solution for a single injection site (red) in COMSOL is in close agreement with the analytical solution for heating from a point source (blue) of equal total power out.

Validation of the Specific Absorption Rate Model to the actual physics of nanoparticle injection and particle distribution is still an emerging area of research in the literature and beyond the scope of this study [3,4,5,7].

5. Conclusion and Design Recommendations

From the results, we see that our model can indeed be used to predict the optimal spatial distribution of injection sites for nanoparticle hyperthermia cancer treatment. Optimizing injection site locations greatly increased the precision of the heating, effectively targeting tumor tissue while minimizing damage to surrounding healthy tissue. The comparison of the SAR model with the analytical solution for heating from a point source has shown that the model produces valid physical results, and thus we can expect the modeling of our tumor hyperthermia to be equally valid.

In order to increase the relevance and utility of our model, several issues must be addressed. First, although the SAR model has been shown to be valid, future experimentation is necessary to correlate A and r_o to physical parameters such as injection rate, injection volume, injection density, and magnetic field strength/frequency. This is especially important for r_o since it was our most sensitive parameter. Second, we could improve upon the SAR model by modeling the actual diffusion of the nanoparticles followed by magnetic heating. This could broaden the possible applications of this model, allowing for modeling of processes such as drug delivery via nanoparticles. Modeling nanoparticle diffusion would require us to account for other phenomena such as deposition effects and electrostatic interaction between particles and tissue.

Our model has several realistic constraints as well. In terms of health safety, our model could be improved. For example, we placed a relative importance of killing tumor tissue to keeping healthy tissue undamaged at a 10:1 ratio in our objective function. In reality, this ratio should be much higher, since leaving detectable amounts of tumor tissue undestroyed would undermine the treatment altogether and render it ineffective. Also, we considered cell death to occur when tissue temperatures reached 43 °C. It would be more accurate to require the tissue to be maintained at a given temperature for a certain amount of time before considering it to be completely killed. These more rigorous requirements would undoubtedly result in greater healthy tissue damage and less picturesque final solutions, but would likely improve the prognoses of the cancer treatments in the long run.

Economic constraints are another barrier in this design. First, we need to consider the cost of further research to characterize nanoparticle distribution as a function of the aforementioned physical parameters. Second, in order for this treatment to work properly, an accurate three dimensional image of the tumor with high spatial resolution is needed. This can be obtained using a high resolution MRI machine, but will incur high costs. Similarly, high resolution imaging is needed not only for obtaining accurate tumor geometry, but also in the actual surgical procedure. In order to inject nanoparticles at specific locations on the order of millimeters, real time imaging with high resolution would be needed to guide the surgical device to the correct location. Further costs would arise from the fact that the surgery would need to be performed by a highly trained surgeon.

Despite these constraints, nanoparticle hyperthermic treatment is a developing technology that has the potential to improve the current methodology of treating cancer and improve the prognoses of individuals with cancer. Further research is required to more accurately model the actual physical processes involved before it is ready for clinical use.

Appendix A

Governing Equations:

2-D Heat transfer equation with volumetric heat generation from multiple injection sites:

$$k \left(\frac{\partial^2 T}{\partial x^2} + \frac{\partial^2 T}{\partial y^2} \right) + \sum_{i=1}^n Q_i = \frac{\partial T}{\partial t}$$

3-D form of previous equation:

$$k \left(\frac{\partial^2 T}{\partial x^2} + \frac{\partial^2 T}{\partial y^2} + \frac{\partial^2 T}{\partial z^2} \right) + \sum_{i=1}^n Q_i = \frac{\partial T}{\partial t}$$

Where $Q_i = A_i e^{-r^2/r_0^2}$ and is the volumetric heating source at a point from a single injection site. This heat generation term is known as the specific absorption rate (SAR) and has been shown in literature to model the hyperthermia process [2,3,4]. Here A is the maximum value of the specific absorption rate at the center of injection and r_0 is the dimensional radius that is associated with how far from the injection site heating affects the tissue. We obtained both of these parameters from literature [2,3]. For the 2D model, r is the distance from the center of an injection site at (x_i, y_i) to any location (x, y) in the domain:

$$r = \sqrt{(x - x_i)^2 + (y - y_i)^2}$$

In the 3D model, r is similar but also accounts for the z axis:

$$r = \sqrt{(x - x_i)^2 + (y - y_i)^2 + (z - z_i)^2}$$

Boundary Conditions: Flux = 0 around all edges of the domain

Initial Conditions: $T = 37$ °C everywhere

The boundary and initial conditions are the same in the 2D and 3D models. A flux of 0 around the normal tissue perimeter was chosen as the boundary condition because it was assumed that the tumor was much smaller in size compared to the surrounding tissue and thus very little heat would diffuse to the outer boundary. This assumption was valid through the relatively short time interval that was simulated in COMSOL. An initial temperature of 37 °C was used to replicate regular internal body temperature.

Table 1: Input parameters for the specific absorption rate heating model and tumor tissue. All parameters were obtained from Salloum et al [2].

A (W/m ³)	1.91E6
r _o (m)	3.1E-3
k (W/m·K)	0.5 (normal) 0.55 (tumor)
c _p (J/kg·K)	4200
ρ (kg/m ³)	1000

Appendix B

The 2D transient heat transfer by conduction model was solved using a direct UMFPACK linear system solver. The time step was fixed at a 1 second interval and the model was simulated for 120 seconds. Calculations were performed using a relative tolerance of 0.01 and absolute tolerance of 0.001.

In the 3D model, the transient heat transfer by conduction equation was solved in COMSOL using the conjugate gradients linear system solver. Time stepping was set at a 1 second interval for a total simulation of 600 seconds. Values for relative tolerance and absolute tolerance were set to 0.01 and 0.001 respectively.

2D and 3D Mesh

We created our mesh using the free mesh parameter method. We anticipated the temperature to vary greatly near the nanoparticle injection sites, so we specified COMSOL to have a smaller mesh element size immediately around the injection sites. Similarly, we specified a smaller mesh size around the tumor-normal tissue border because we wanted to make the temperature profile at this border as precise as possible. In 2D, our entire mesh consisted of 19249 elements, as shown by Figure 8.

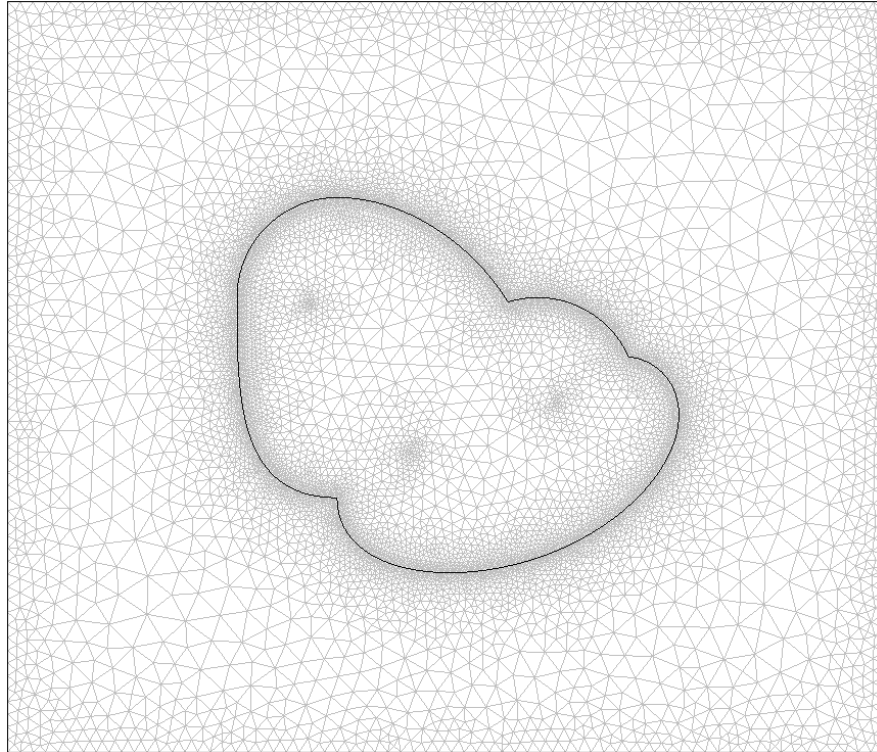


Figure 8: Mesh (grey lines) for the 2D tumor geometry. The black line indicates the border between tumor (inside) and normal (outside) tissue.

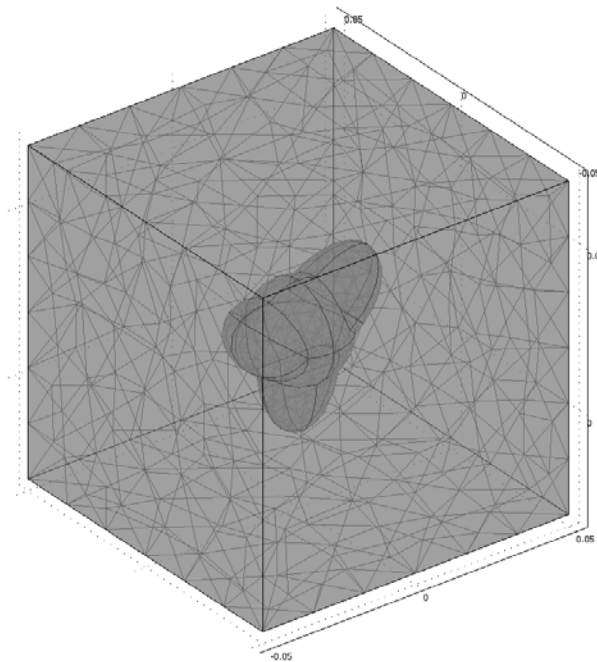


Figure 9: 3D tumor geometry mesh with 10861 elements. Free mesh with coarse predefined element sizes was utilized in this diagram.

The 3D geometry (Figure 9) was created in COMSOL out of 3 ellipsoids and 1 sphere to imitate tumor geometries in vivo [2,3]. Injection sites were initially chosen to be at the center of each ellipsoid and the center of the sphere.

We performed mesh convergence on the 3D geometry using the default free mesh. The temperature was evaluated at the tumor center and outer most points on each tumor arm. Convergence occurred by 38000 elements so this mesh was used for the remainder of the analysis. Computation time was on the scale of tens of seconds.

Mesh Convergence Analysis

Figure 10 shows that using a finer mesh near the boundaries and injection sites is not necessary since both types of meshes provide similar results. Since the computation time does not increase much even with a higher number of elements, the finer mesh was still used since it produced plots with better resolution.

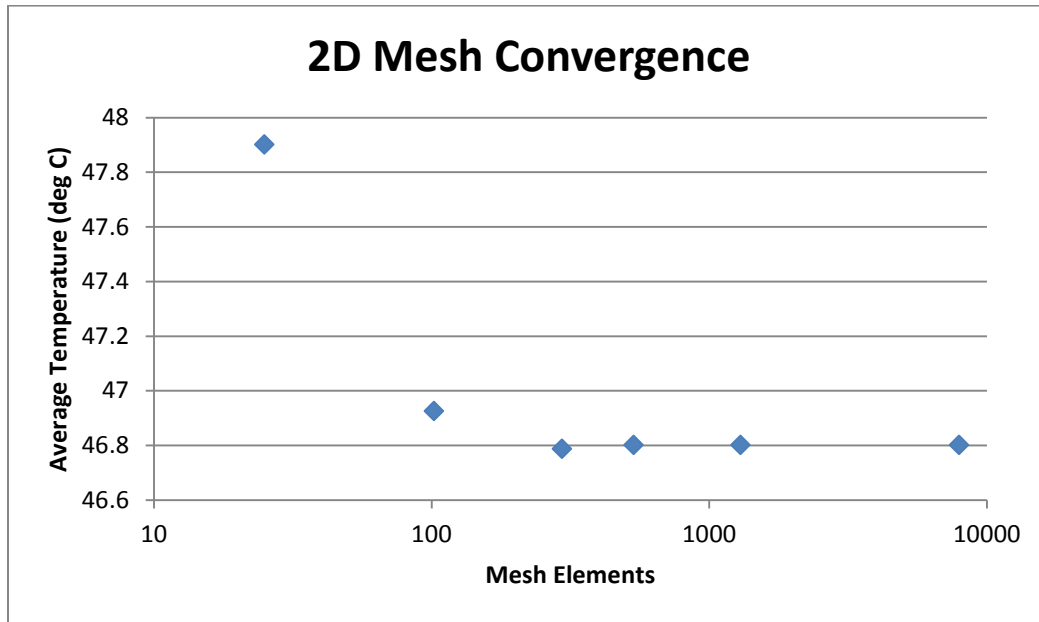


Figure 10: Mesh convergence plot of the average tumor temperature. Average temperature does not change much after 295 mesh elements.

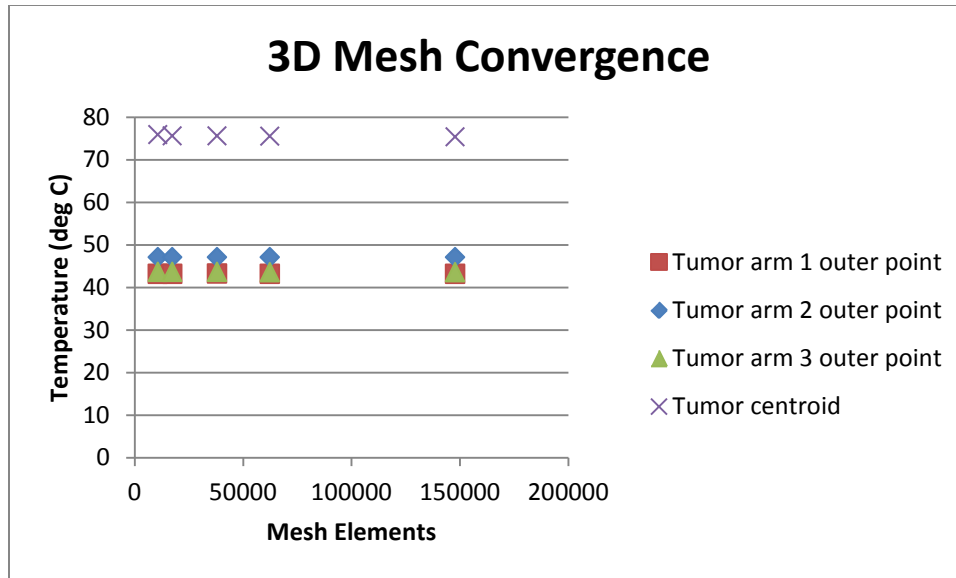


Figure 11: 3D Mesh convergence plot. Temperature at the end of each of tumor arm does not change with increasing element size.

Temperature convergence was tested at different points instead of taking the average temperature of the whole tumor in the 3D model due to a greater degree of temperature variation that occurred within the 3D tumor (Figure 11). Convergence occurs even at a low number of mesh elements.

Appendix C

References

1. American Cancer Society. Cancer Facts & Figures 2012. Atlanta: American Cancer Society; 2012. <<http://www.cancer.org/acs/groups/content/@epidemiologysurveillance/documents/document/acspc-031941.pdf>>
2. Salloum, M. et al. *Enhancement in treatment planning for magnetic nanoparticle hyperthermia: Optimization of the heat absorption pattern*. J. Hyperthermia. 2009. **25**(4): p. 309-321.
3. Attaluri, A. et al. *Nanoparticle distribution and temperature elevations in prostatic tumours in mice during magnetic nanoparticle hyperthermia*. Int. J. Hyperthermia. 2011. **27**(5): p. 421-502.
4. Su, D. et al. *Multi-scale study of nanoparticle transport and deposition in tissues during an injection process*. Med Biol Eng Comput. 2010. **48**: p. 853-863.
5. Golneshan, A., Lahonian, M. *The effect of magnetic nanoparticle dispersion on temperature distribution in a spherical tissue in magnetic fluid hyperthermia using the lattice Boltzman method*. Int. J. Hyperthermia. 2011. **27**(3): 266-274
6. Yamada, K. et al. *Minimally required heat doses for various tumour sizes in induction heating cancer therapy determined by computer simulation using experimental data*. Int. J. Hyperthermia. 2010. **26**(5): 465-474
7. Attaluri, A. et al. *Using MicroCT imaging technique to quantify heat generation distribution induced by magnetic nanoparticles for cancer treatments*. Journal of Heat Transfer. 2011. 133:011003